RSC Advances

PAPER

View Article Online
View Journal | View Issue

Cite this: *RSC Adv.*, 2016, **6**, 65377

Low temperature hydrogenation of α-angelica lactone on silica supported Pd–NiO catalysts with synergistic effect†

Pei Zhang, Qingqing Yuan, Li Chen, Teng Xue, Yejun Guan* and Peng Wu

Received 23rd May 2016
Accepted 30th June 2016

DOI: 10.1039/c6ra13374f

www.rsc.org/advances

The hydrogenation of α-angelica lactone (α-AL) was achieved under mild conditions on silica supported Pd–NiO catalysts. NiO and palladium were sequentially loaded on silica by wet-impregnation and deposition–reduction, respectively. First a series of NiO/SiO_2 supports with varying Ni contents were prepared by a wet-impregnation method with $Ni(NO_3)_2$ as the precursor followed by calcination in air. Then a minute amount of palladium (0.2 wt%) was loaded by a deposition–reduction method using $NaBH_4$ as a reducing reagent. The Pd–NiO catalysts were characterized by nitrogen adsorption, XRD, H_2-TPR, XPS and TEM. The NiO were heterogeneously dispersed on silica with particle sizes ranging from 10 to 50 nm, whereas Pd was finely loaded with a diameter less than 5 nm. Nanoscale intimacy between Pd and NiO was noticed by HRTEM, resulting in high catalytic activity in liquid phase hydrogenation of α-angelica lactone to γ-valero lactone (GVL) under mild conditions. 0.2Pd–9.9NiO/SiO_2 showed the best activity among all the catalysts investigated, with 82% conversion and 100% selectivity to GVL within several minutes at 30 °C and 0.3–1 MPa H_2 pressure.

Introduction

As a kind of promising composite material, bimetal catalysts have been intensively studied in recent years due to the well-known synergistic effect which will not be present in corresponding monometallic catalysts.[1–8] From a practical point of view, the use of a bimetal catalyst is an interesting strategy as it offers many possibilities such as an increase of catalytic activity and tuning of the selectivity, especially as observed in upgrading biomass to chemicals and fuels.[9–13] Precious metals, such as palladium, have been widely used in catalytic hydrogenation processes. When combined with a second transition metal, such as nickel, enhanced reactivity and/or selectivity can be achieved in many hydrogenation reactions.[14–21] Nakagawa and co-workers[14] reported the hydrogenation of 5-hydroxymethyl-2-furaldehyde by Ni–Pd bimetallic catalysts supported on silica (Ni/Pd = 7). The yield of 2,5-bis(hydroxymethyl)tetrahydrofuran reached 96% over bimetallic catalysts, which was more active than commercial RANEY® Ni and more selective than Pd/C. Yang *et al.*[16] have introduced a new procedure for the reduction of aromatic nitro compounds into amines with Pd/NiO-MC (Ni-doped monolithic carbon aerogels) catalysts under ambient conditions (25 °C, 1 atm H_2). Recently, Liu *et al.*[18] reported that Pd–NiO@SiO_2 nanocatalysts illustrated an excellent catalytic performance for catalytic *p*-chloronitrobenzene (*p*-CNB) hydrogenation (full conversion, 82.7% selectivity of *p*-chloroaniline). The conversion of *p*-CNB over different catalyst followed the trend of Pd–NiO@SiO_2 > Pd@SiO_2 > PdNi@SiO_2. Synergistic effect between nickel or nickel oxide and palladium has been proposed to explain the unique catalytic behavior of these catalysts.[12,18] Inspired by these studies, we herein reported the hydrogenation performance of the Pd–NiO catalyst with minute amount of Pd (0.2 wt%).

α-AL has been defined as a new potential platform molecule which can be produced from lignocellulosic materials levulinic acid (LA) by dehydration (Scheme 1).[22] As a perfume or food additive, α-AL is widely used in the food and tobacco industry. Moreover, it can serve as a fuel blending agent or a precursor for the preparation of γ-valerolactone (GVL), 2-methyltetrahydrofuran (2-MTHF) and levulinic acid esters. GVL is such a platform chemical that offers tremendous flexibility in downstream applications.[23] It has been successfully used for the production of ionic liquids,[24] butenes,[25] 1,4-pentanediols and alkanes,[26] *etc.* There have been extensive studies about the hydrogenation LA and/or ethyl levulinate (EL) to produce GVL.[27–34] Compared with

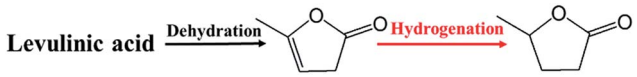

Scheme 1 The synthesis of GVL from levulinic acid *via* α-angelica lactone as an intermediate.

Shanghai Key Laboratory of Green Chemistry and Chemical Processes, School of Chemistry and Chemical Engineering, East China Normal University, North Zhongshan Road 3663, 200062, Shanghai, China. E-mail: yjguan@chem.ecnu.edu.cn

† Electronic supplementary information (ESI) available. See DOI: 10.1039/c6ra13374f

LA or EL, α-AL can be hydrogenated smoothly under mild conditions over both Pd and Ru catalysts.[22,35] Zhang *et al.* have reported the conversion of α-AL to GVL at 60 °C and 4.0 MPa H_2 pressure using 10 wt% Pd/C catalyst in a series of ionic liquids. Among these ionic liquids, [Bmim]PF_6 showed the best performance on the selectivity of GVL (99.8%). However, some ionic liquids are in solid phase at room temperature and difficult to form a homogeneous solution with the reactant as a result of low conversion. In another study, Al-Shaal *et al.*[35] found that the GVL yield exceeded 97% with full conversion of α-AL under moderate reaction conditions (50 °C, 24 bar H_2 pressure for 1 h or room temperature, 500 mL min^{-1} H_2-flow rate for 24 h) over Ru/C catalyst. These results indicated that noble metals (Pd or Ru species) are able to saturate C=C bonds easily under mild reaction conditions. Herein, we showed that fast hydrogenation of α-AL can be achieved on a silica supported Pd–NiO catalyst with minute amount of Pd (0.2 wt%) under mild conditions.

Experimental

Preparation of catalysts

NiO-bulk. NiO-bulk was prepared by calcination of the $Ni(NO_3)_2 \cdot 6H_2O$ at 500 °C for 1 h in air.

***x*NiO–SiO_2.** *x*NiO–SiO_2 (*x* = 0.26, 2, 9.9, 19, 29 and 40 determined by ICP, wt%) samples were prepared by wet-impregnation method followed by calcination at 500 °C in air for 1 h. The SiO_2 used was Evonik Degussa Aerosil® 200 with surface area of 208 m^2 g^{-1}.

Supported Pd catalysts. Supported Pd catalysts (~0.2 wt%, determined by ICP) were prepared by a typical deposition–precipitation–reduction method.[36] The support (0.3 g) was dispersed in H_2O (60 mL) with stirring. A specified amount of H_2PdCl_4 aqueous solution (21.512 g_{Pd} L^{-1}) was added to the mixture and stirred for 3 h. The final pH value of the suspension was adjusted to 10 by adding NaOH solution (1 M). Then, $NaBH_4$ aqueous solution ($NaBH_4$/Pd = 10, molar ratio) was added into the suspension and the mixture was stirred for another 30 min allowing for the full reduction of Pd^{2+} species. Thus obtained catalyst was dried at 110 °C overnight. The sample was denoted as Pd–*x*NiO–SiO_2 (*x* stands for Ni loading).

Catalyst characterization

Nitrogen adsorption–desorption isotherms at −196 °C were obtained on a BELSORP-Max equipment. Prior to the measurement, the samples were first degassed at 150 °C under vacuum for 6 h. Specific surface areas (SSA) were calculated by the Brunauer–Emmett–Teller (BET) method using five relative pressure points in the interval of 0.05–0.30. The pore size distribution was obtained by the Barrett–Joyner–Halenda (BJH) model applied to the adsorption isotherm.

The Pd loading was quantified by inductively coupled plasma (ICP) on a Thermo IRIS Intrepid II XSP atomic emission spectrometer. About 25 mg catalysts were digested using 5 mL of aqua regia. The obtained solutions were diluted with deionized water to the desired Pd concentration.

The power X-ray diffraction (XRD) patterns were collected on a Rigaku Ultima IV X-ray diffractometer using Cu Kα radiation (λ = 1.5405 Å) operated at 35 kV and 25 mA. Transmission electron microscopy (TEM) images were taken on a FEI Tecnai G^2 F30 microscope operating at 300 kV.

Temperature programmed reduction (TPR) measurements were carried out in TP-5080 (Tianjin Xianquan, China) equipped with a thermal conductivity detector (TCD). The calcined samples were treated at 100 °C for 30 min under He stream (25 mL min^{-1}) for 1 h in order to remove the physisorbed water. Then the samples were cooled down to 25 °C in the same atmosphere, and were heated up to 630 °C at 10 °C min^{-1} in a 5% (v/v) hydrogen/nitrogen flow.

The X-ray photoelectron spectroscopy (XPS) was recorded on an Escalab 250xi spectrometer, using a standard Al Kα X-ray source (300 W) and analyzer pass energy of 30.0 eV. All binding energies were referenced to the adventitious C 1s line at 284.6 eV.

Catalytic tests

The catalytic hydrogenation was conducted in a Teflon-lined (60 mL) steel batch reactor. 25 mg of catalyst was loaded into the reactor along with 9.8 mL of H_2O and 0.2 mL of substrate. No pretreatment on the catalysts was conducted prior to reaction. The reactor was purged with H_2 for five times and then pressurized with 0.3 MPa H_2. The mixture was stirred in a water-bath at 30 °C. The products were diluted with ethanol and analyzed with flame ionization detector (FID) and capillary column of DB-FFAP (30 m length and 0.25 mm internal diameter).

Results and discussion

Characterization of supported catalysts

The textural properties of the supported catalysts are shown in Table 1. The surface area of SiO_2 is 208 m^2 g^{-1}. As can be seen, deposition of 0.2 wt% Pd caused a slight decrease in the specific surface (from 208 to 192 m^2 g^{-1}). With the NiO loading increased (from 0.26 to 19.9 wt%), the surface area reduced substantially (from 197 to 149 m^2 g^{-1}). These can be explained by the introduction of large amount of NiO particles into the SiO_2 pores.

Fig. 1 shows the XRD patterns of Pd–*x*NiO/SiO_2. The diffraction peaks located at 37, 43, 63, 75, and 79° are assigned to the NiO phase [JCPDS 44-1159]. The intensity of these peaks

Table 1 Textural properties of supports and supported Pd catalysts

Catalysts	SSA (m^2 g^{-1})	Pore volume (cm^3 g^{-1})
SiO_2	208	0.8
NiO	5.5	0.078
Pd–SiO_2	192	0.65
Pd–0.26NiO/SiO_2	197	0.64
Pd–2NiO/SiO_2	183	0.67
Pd–9.9NiO/SiO_2	166	0.55
Pd–19NiO/SiO_2	149	0.44

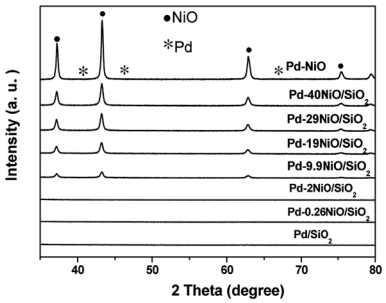

Fig. 1 XRD patterns of Pd–xNiO–SiO_2 catalysts.

became weakened with the decrease of NiO loading. In all cases, no Pd diffraction peaks were observed, meaning that Pd nanoparticles were highly dispersed on metal supports or the diffraction intensity was beyond the detection limit at very low Pd loading (0.2 wt%).

Fig. 2 shows the TPR profiles of the NiO/SiO_2 and Pd–xNiO/SiO_2 samples. The reduction profile of crystalline NiO prepared by calcining $Ni(NO_3)_2 \cdot 6H_2O$ at 500 °C showed temperature maximum (T_{max}) at 408 °C. This result is in agreement with earlier reports.[37–41] $9.9NiO/SiO_2$ and $2NiO/SiO_2$ presented broad reduction peak with T_{max} of 388 and 418 °C, respectively. The lower T_{max} of $9.9NiO/SiO_2$ is likely assigned to those easily reducible nickel oxide particles with large crystallites or those weakly interacting with the support.[37] Pd–$2NiO/SiO_2$ and Pd–$9.9NiO/SiO_2$ had their T_{max} at 371 °C and 381 °C, respectively. This result reveals that the presence of trace amount of Pd species enhanced the reduction of NiO. Moreover, the negative peak due to palladium β-hydride phase as commonly observed in H_2-TPR profile of Pd/SiO_2 (Fig. S2†) disappeared on Pd–NiO catalysts. This phenomenon certainly suggests the strong interaction between Pd and NiO, as has been reported earlier on PdFe catalysts.[42]

We studied by XPS the surface Pd and Ni species for Pd–$9.9NiO/SiO_2$. The Pd 3d and Ni 3p spectra were fitted and the results are shown in Fig. 3. NiO species were clearly found in Pd–$9.9NiO/SiO_2$ according to the binding energies located at 854.7, 856.3 and 861.1 eV (Fig. 3a).[43–45] Oxidized Pd^{2+} (Fig. 3b) species were observed for this sample (binding energies of 337.2 and 342.0 eV), which is likely due to the exposure of Pd

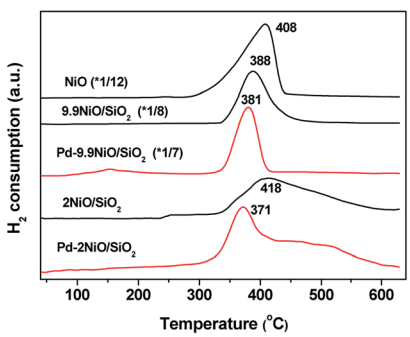

Fig. 2 H_2-TPR profiles of NiO-bulk, $2NiO/SiO_2$, $9.9NiO/SiO_2$, 0.2Pd–$2NiO/SiO_2$ and 0.2Pd–$9.9NiO/SiO_2$ catalysts.

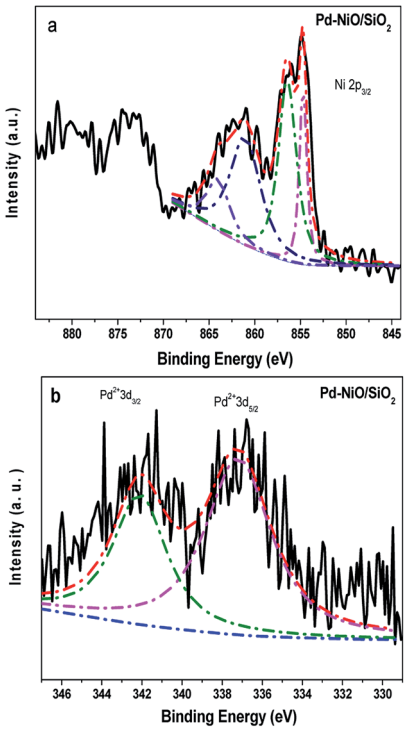

Fig. 3 X-ray photoelectron spectra fitting of (a) Ni $2p_{3/2}$ and (b) Pd 3d of Pd–$9.9NiO/SiO_2$.

nanoparticle in air.[46] The accurate distribution of Pd and NiO on Pd–$9.9NiO/SiO_2$ was further examined by HRTEM, high-angle annular dark field scanning tunneling electron microscopy (HAADF-STEM) (Fig. 4). From Fig. 4a and b one can see that irregular spherical particles were well dispersed on the SiO_2 support. HRTEM images reveal the presence of two types of lattice spacing due to Pd nanoparticles: 0.22 and 0.19 nm assigned to Pd (111) and Pd (200) plane, respectively.[18,47,48] These Pd nanoparticles were found to be closely attached on a (220) surface of NiO particles with lattice spacing about 0.14–0.15 nm.[16] To get more insight on the spatial distribution of Pd

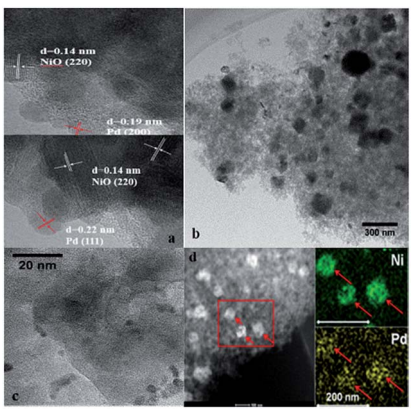

Fig. 4 TEM images of (a) high resolution and (b) low resolution of Pd–$9.9NiO–SiO_2$; (c) Pd–$9.9NiO–SiO_2$-reused; (d) HAADF-STEM-EDX mapping images of the Pd–$9.9NiO/SiO_2$.

and NiO, HAADF-STEM along with high resolution elemental mapping was undertaken. The mapping results indicated that NiO (shown by green dots) and Pd (shown by yellow dots) located in exactly the same zone. These results lead to the conclusion that palladium closely interacted with NiO in a big chance, which is consistent with the TPR results.

Catalytic activities of supported Pd catalysts

Table 2 summarizes the catalytic performance of NiO/SiO_2, Pd/SiO_2, and $Pd–NiO/SiO_2$ catalysts in the hydrogenation of α-AL under 0.3 or 1 MPa H_2 pressure. For comparison, SiO_2 (Table 2, Entry 1) and $NiO–SiO_2$ (Table 2, Entry 2) were tested and both supports did not show any catalytic activity under 0.3 MPa H_2. Increasing the H_2 pressure to 1 MPa led to the production of minute amount of β-AL (Table 2, Entry 3) due to the isomerization of α-AL catalyzed by acid sites. It is likely that certain amount of acid sites related to Ni–OH species might be formed at high H_2 pressure, which favors the isomerization reaction pathway. Nevertheless, $NiO–SiO_2$ was not active at all for the hydrogenation of α-AL under mild conditions. When 0.2 wt% Pd was supported on SiO_2, the α-AL conversion after 1 h was 29% with GVL selectivity being 95% (Table 2, Entry 4). This result demonstrates that Pd species were very active for the hydrogenation of C=C bond in α-AL molecule even supported on an inert support such as SiO_2. When supported on an active support, namely bulk NiO, the α-AL conversion was 76% after 0.5 h with enhanced GVL selectivity as 100% (Table 2, Entry 5). This result points to the synergy between Pd and NiO in hydrogenation reactions, which is most likely related to the structure modification of Pd metal by the addition of NiO.

Due to the low surface area (5.5 $m^2 g^{-1}$) and high cost of bulk NiO, we next tested the activity of Pd supported on $NiO–SiO_2$ with high surface area and low Ni content. The result (Table 2, Entry 6) showed that for $Pd–9.9NiO/SiO_2$, the conversion of α-AL after 30 min and selectivity of GVL was 82% and 100%, respectively. This reactivity was equal to or slightly higher than Pd supported on bulk NiO. As expected, the inert SiO_2 with relatively larger specific surface area could disperse NiO particles very well so that more Pd–NiO active sites were provided. Further increase of NiO content did not lead to improved α-AL conversion (Table 2, Entry 7).

To clarify the role of Pd–NiO in facilitating α-AL hydrogenation, we thus performed a set of control experiments. First we tested the hydrogenation activity of physical mixture of Pd/SiO_2 and $9.9NiO/SiO_2$ (each in 15 mg catalyst). The conversion of α-AL was 12% after 1 h with GVL selectivity of 70% (Table 2, Entry 9). This result showed that a nanoscale intimacy of Pd and NiO was the prerequisite to achieve the high hydrogenation activity of α-AL. Second we pre-reduced the $Pd–9.9NiO/SiO_2$ in H_2 flow and tested its hydrogenation activity (Table 2, Entry 10). The results clearly suggested that the reduction of Pd–NiO led to dramatic drop of α-AL conversion (27%). This unexpected result prompted us to test the catalytic activity of $Pd–Ni/SiO_2$ catalyst in this reaction.

A series of Ni/SiO_2 supports were prepared (see ESI†) by reducing the NiO/SiO_2 supports in flowing H_2 and then Pd was loaded *via* the same deposition–reduction method as $Pd–NiO/SiO_2$ catalysts. We compared the turnover frequencies (TOF, based on α-AL conversion per Pd weight) of Pd nanoparticles supported on NiO/SiO_2 and Ni/SiO_2 (Fig. 5). It should be noted that in order to achieve a reliable TOF, the conversion of α-AL

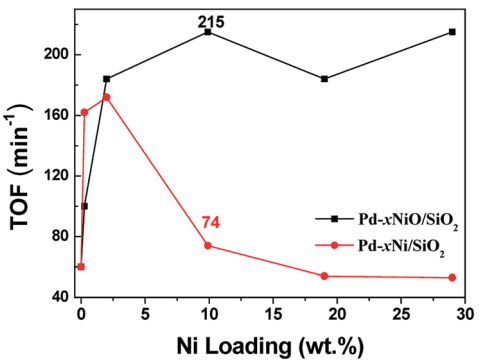

Fig. 5 TOF values, defined as mol_{GVL} $(mol_{Pd}\ min)^{-1}$, of $Pd–xNiO/SiO_2$ and $Pd–xNi/SiO_2$ in α-AL hydrogenation.

Table 2 Catalytic activity of supported Pd catalysts in α-AL hydrogenation[a]

Entry	Catalyst	Time (min)	H_2 pressure (MPa)	Conv. (%)	Sel.% GVL	Sel.% β-AL
1	SiO_2	60	0.3	—	—	—
2	$9.9NiO–SiO_2$	60	0.3	—	—	—
3	$9.9NiO–SiO_2$	60	1	1	—	100
4	$Pd–SiO_2$	60	0.3	29	95	5
5	Pd–NiO-bulk	30	0.3	76	100	—
6	$Pd–9.9NiO/SiO_2$	30	0.3	82	100	—
7	$Pd–40NiO/SiO_2$	30	0.3	78	100	—
8	$Pd–40Ni/SiO_2$	30	0.3	20	100	—
9	NiO/SiO_2 + Pd/SiO_2[b]	60	0.3	12	70	30
10	Pre-reduced-$Pd–9.9NiO/SiO_2$[c]	30	0.3	27	100	—

[a] Reaction conditions: catalyst (25 mg), H_2O (9.8 mL), α-AL (0.2 mL), 30 °C. [b] Physical mixture: 15 mg of NiO/SiO_2 and 15 mg of Pd/SiO_2. [c] Catalyst was pretreated with H_2 at 200 °C for 10 min, cooled down to room temperature under N_2 flow, and then the reaction solution was added immediately.

has been controlled to be below or close to 30%. For catalysts with high Ni loading, for instance Pd–40Ni/SiO_2, the α-AL conversion was 20% after 1 h (Table 2, Entry 8), which was much lower than that of Pd–40NiO/SiO_2 (78% after 0.5 h, Table 2, Entry 7). Metallic Ni significantly suppressed the hydrogenation activity of Pd nanoparticles supported thereof. Surprisingly, no significant difference in TOF between Pd–2Ni/SiO_2 and Pd–2NiO/SiO_2 was observed. At this stage we cannot give a convincible explanation for this catalysis behavior. It might because the influence of metal Ni on the hydrogenation activity of Pd is rather weaker comparing with that of surface NiO when Ni loading is low.

Based on these results, we try to explain the pathways of α-AL hydrogenation by taking into account of previous reports.[22,35] At the initial stage of the reaction, isomerization of α-AL to β-AL might occur (Table 2, Entry 3). Then, concerted adsorption of C=C bond of α(and/or β)-AL and hydrogen takes place on neighbored Pd atoms and NiO surface. After the saturation of C=C bonds by nearby hydrogen atoms, the formed GVL molecules desorbs to the liquid phase. It should be noted that another possible reaction mechanism cannot be excluded, wherein NiO acts as the adsorption sites of α-AL and Pd activates hydrogen. The hydrogenation is then accomplished on NiO *via* the H-spillover mechanism. Additionally, we tried to reveal the reaction kinetic by testing the hydrogenation performance of Pd–9.9NiO/SiO_2 catalyst under different experiment conditions (Table S1†). The results showed that the hydrogenation rate was nearly zero order in lactone and first order in hydrogen. This indicated that the Pd–NiO surface was largely covered with unsaturated molecules, whereas hydrogen was only weakly adsorbed.

Catalyst reusability

The reusability of Pd–9.9NiO/SiO_2 and Pd/SiO_2 catalyst was evaluated through six repeated reactions. After the first run, the catalyst was separated through centrifugation, thoroughly washed and then dried at 60 °C before the next use. The activity in terms of α-AL conversion and GVL selectivity is shown in Fig. 6. It can be clearly seen that Pd–9.9NiO/SiO_2 catalyst showed very stable reactivity in the first five runs and starts to deactivate in the next run. TEM image of the reused catalyst (Fig. 4c) suggested no significant aggregation of Pd nanoparticles. Elemental analysis (ICP) of the reused catalyst revealed that no leaching of Pd occurred (not shown) either. However, we noticed that the catalyst particles became badly dispersed in the aqueous solution after 6 runs, leading to strong diffusion limitations of substrates. Compared with Pd–9.9NiO/SiO_2, the selectivity of GVL on Pd/SiO_2 started decreasing already in the second run and decreased from 95% to 66% in the 6th run, which implying the hydrogenation activity loss of Pd in hydrogenation.

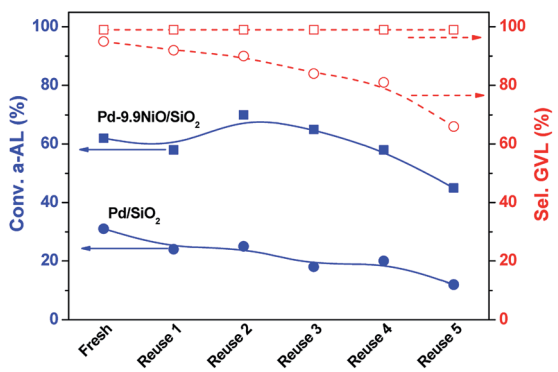

Fig. 6 Recycle study of Pd–9.9NiO/SiO_2 (Conv. (■) and sel. to GVL (□)) and Pd/SiO_2 (Conv. (●) and sel. to GVL (○)) for α-AL hydrogenation. Reaction conditions: 0.4 mL of α-AL, 50 mg of catalyst, 4 mL of H_2O, 30 °C, 25 min, 0.3 MPa H_2.

Conclusions

We demonstrated that the hydrogenation of α-AL to GVL can be successfully performed under mild conditions over a series of Pd–*x*NiO/SiO_2 a with very low Pd loading (0.2 wt%). Amongst the catalysts investigated, Pd–9.9NiO–SiO_2 was the most active one and it could be reused at least six times without Pd leaching. Pd–O–Ni species formed by the intimate interaction between Pd and NiO tend to be the active site on Pd–*x*NiO/SiO_2 catalysts in H_2 activation and the following C=C saturation. The hydrogenation rate with respect to the α-AL and hydrogen pressure is nearly zero order and first order, respectively. Our results suggest that it is possible to achieve very high hydrogenation activity while using minute amount of Pd with the aid of a second cheap transition metal oxide in the conversion of biomass-derived oxygenates.

Acknowledgements

We acknowledge the financial support from the National Natural Science Foundation of China (Grants No. 21203065 and 21533002).

Notes and references

1 D. M. Alonso, S. G. Wettstein and J. A. Dumesic, *Chem. Soc. Rev.*, 2012, **41**, 8075.
2 C. Bernard and F. François, *Coord. Chem. Rev.*, 1998, **178–180**, 1753.
3 C. Bernard and F. François, *J. Mol. Catal. A: Chem.*, 2001, **173**, 117.
4 Z. Wei, J. Sun, Y. Li, A. K. Datye and Y. Wang, *Chem. Soc. Rev.*, 2012, **41**, 7994.
5 M. Sankar, N. Dimitratos, P. J. Miedziak, P. P. Wells, C. J. Kiely and G. J. Hutchings, *Chem. Soc. Rev.*, 2012, **41**, 8099.
6 F. Riccardo, J. Julius and L. J. Roy, *Chem. Rev.*, 2008, **108**, 846.
7 C. Liu, X. Li and T. Wang, *RSC Adv.*, 2015, **5**, 57277.
8 L. Zhu, J. Zheng, C. Yu, N. Zhang, Q. Shu, H. Zhou, Y. Li and B. H. Chen, *RSC Adv.*, 2016, **6**, 13110.
9 G. W. Huber, J. W. Shabaker, S. T. Evans and J. A. Dumesic, *Appl. Catal., B*, 2006, **62**, 226.
10 J. W. Shabaker, G. W. Huber and J. A. Dumesic, *J. Catal.*, 2004, **222**, 180.

11 J. Lee, Y. T. Kim and G. W. Huber, *Green Chem.*, 2014, **16**, 708.
12 B. Chen, F. Li, Z. Huang and G. Yuan, *Appl. Catal., A*, 2015, **500**, 23.
13 D. J. M. de Vlieger, A. G. Chakinala, L. Lefferts, S. R. A. Kersten, K. Seshan and D. W. F. Brilman, *Appl. Catal., B*, 2012, **111–112**, 536.
14 Y. Nakagawa and K. Tomishige, *Catal. Commun.*, 2010, **12**, 154.
15 N. S. Babu, N. Lingaiah and P. S. S. Prasad, *Appl. Catal., B*, 2012, **111–112**, 309.
16 H. Yang, X. Cui, Y. Deng and F. Shi, *ChemCatChem*, 2013, **5**, 1739.
17 T. Jiang, Q. Huai, T. Geng, W. Ying, T. Xiao and F. Cao, *Biomass Bioenergy*, 2015, **78**, 71.
18 H. Liu, K. Tao, C. Xiong and S. Zhou, *Catal. Sci. Technol.*, 2015, **5**, 405.
19 W. Huang, J. McCormick, R. Lobo and J. Chen, *J. Catal.*, 2007, **246**, 40.
20 Y. Huang and M. H. S. Wolfgang, *J. Catal.*, 1999, **188**, 215.
21 Y. Wang, X. Cui, Y. Deng and F. Shi, *RSC Adv.*, 2014, **4**, 2729.
22 R. Cao, J. Xin, Z. Zhang, Z. Liu, X. Lu, B. Ren and S. Zhang, *ACS Sustainable Chem. Eng.*, 2014, **2**, 902.
23 D. M. Alonso, S. G. Wettstein and J. A. Dumesic, *Green Chem.*, 2013, **15**, 584.
24 D. Fegyverneki, L. Orha, G. Lang and I. T. Horvath, *Tetrahedron*, 2010, **66**, 1078.
25 J. Q. Bond, D. M. Alonso, D. Wang, R. M. West and J. A. Dumesic, *Science*, 2010, **327**, 1110.
26 H. Mehdi, V. Fábos, R. Tuba, A. Bodor, L. T. Mika and I. T. Horváth, *Top. Catal.*, 2008, **48**, 49.
27 (*a*) K. Kon, W. Onodera and K. Shimizu, *Catal. Sci. Technol.*, 2014, **4**, 3227; (*b*) F. Liguori, C. Moreno-Marrodan and P. Barbaro, *ACS Catal.*, 2015, **5**, 1882; (*c*) W. R. H. Wright and R. Palkovits, *ChemSusChem*, 2012, **5**, 1657.
28 V. V. Kumar, G. Naresh, M. Sudhakar, J. Tardio, S. K. Bhargava and A. Venugopal, *Appl. Catal., A*, 2015, **505**, 217.
29 M. Sudhakar, V. V. Kumar, G. Naresh, M. L. Kantam, S. K. Bhargava and A. Venugopal, *Appl. Catal., B*, 2016, **180**, 113.
30 H. Heeres, R. Handana, D. Chunai, C. B. Rasrendra, B. Girisuta and H. J. Heeres, *Green Chem.*, 2009, **11**, 1247.
31 H. Schuette and R. W. Thomas, *J. Am. Chem. Soc.*, 1930, **52**, 3010.
32 R. V. Christian Jr, H. D. Brown and R. M. Hixon, *J. Am. Chem. Soc.*, 1947, **69**, 1961.
33 M. Chia and J. A. Dumesic, *Chem. Commun.*, 2011, **47**, 12233.
34 F. Y. Ye, D. M. Zhang, T. Xue, Y. M. Wang and Y. Guan, *Green Chem.*, 2014, **16**, 3951.
35 M. G. Al-Shaal, P. J. Hausoul and R. Palkovits, *Chem. Commun.*, 2014, **50**, 10206.
36 D. M. Zhang, Y. Guan, E. J. M. Hensen, T. Xue and Y. Wang, *Catal. Sci. Technol.*, 2014, **4**, 795.
37 B. Mile, D. Stirling, M. A. Zammitt, A. Lovell and M. Webb, *J. Catal.*, 1988, **114**, 217.
38 N. W. Hurst, S. J. Gentry, A. Jones and B. D. McNicol, *Catal. Rev.*, 1982, **24**, 233.
39 J. Zielifiski, *Catal. Lett.*, 1995, **31**, 47.
40 G. Li, L. Hu and J. M. Hill, *Appl. Catal., A*, 2006, **301**, 16.
41 C. W. Hu, J. Yao, H. Q. Yang, Y. Chen and A. M. Tian, *J. Catal.*, 1997, **166**, 1.
42 J. K. Kim, J. K. Lee, K. H. Kang, J. W. Lee and I. K. Song, *J. Mol. Catal. A: Chem.*, 2015, **410**, 184.
43 M. C. Biesinger, B. P. Payne, A. P. Grosvenor, L. W. M. Lau, A. R. Gerson and R. S. C. Smart, *Appl. Surf. Sci.*, 2011, **257**, 2717.
44 G. Bai, H. Dai, J. Deng, Y. Liu, W. Qiu, Z. Zhao, X. Li and H. Yang, *Chem. Eng. J.*, 2013, **219**, 200.
45 F. Yu, X. Xu, H. Peng, H. Yu, Y. Dai, W. Liu, J. Ying, Q. Sun and X. Wang, *Appl. Catal., A*, 2015, **507**, 109.
46 D. Zemlyanov, B. A. Kiss, E. Kleimenov, D. Teschner, S. Zafeiratos, M. Havecker, A. K. Gericke, R. Schlogl, H. Gabasch, W. Unterberger, K. Hayek and B. Klotzer, *Surf. Sci.*, 2006, **600**, 983.
47 S. Dutta, C. Ray, S. Mallick, S. Sarkar, A. Roy and T. Pal, *RSC Adv.*, 2015, **5**, 51690.
48 W. Wang, Y. Yang, Y. Liu, Z. Zhang, W. Dong and Z. Lei, *J. Power Sources*, 2015, **273**, 631.